J Mol Model (2009) 15:1271–1280
DOI 10.1007/s00894-009-0491-4

ORIGINAL PAPER

Insights into the high fidelity of a DNA polymerase I mutant

Thomas E. Exner

Received: 8 December 2008 / Accepted: 12 March 2009 / Published online: 31 March 2009

Abstract Mutants of DNA polymerase I from *Thermus aquaticus* (*Taq*) with higher fidelity compared to the wild type enzyme were identified in an earlier study by Summerer et al. (Angew Chem Int Ed 44:4712–4715, 2005). Here, one of these mutants, PLQ (consensus residues 879–881), was analysed using molecular dynamics simulations. This was done by calculating the structures of the ternary complex comprising the enzyme, the DNA primer and template as well as the incoming nucleotide before the chemical reaction for the Watson-Crick and different mismatched base pairings. The results show that the high fidelity of the mutant can be explained partly by different specific interactions between the amino acids of the enzyme and the DNA primer end as well as, in some mismatches, a displacement of the primer relative to the incoming deoxyribonucleoside triphosphate and the catalytic magnesium ion. This displacement is facilitated by reduced steric interactions between the enzyme and the DNA.

Keywords Polymerase mutants · Incorporation · Fidelity · Ternary complex before chemical reaction · Molecular dynamics simulations

Electronic supplementary material The online version of this article (doi:10.1007/s00894-009-0491-4) contains supplementary material, which is available to authorized users.

T. E. Exner (✉)
Department of Chemistry and Zukunftskolleg,
University of Konstanz,
78457 Konstanz, Germany
e-mail: thomas.exner@uni-konstanz.de

Introduction

The accurate replication of DNA is of the utmost importance for the maintenance of genomic integrity. Key players in DNA replication as well as repair synthesis are DNA polymerases, which add deoxynucleotides on to the growing end of a DNA primer strand using a single-stranded DNA as a template. DNA polymerases show a highly conserved structure resembling a hand-like arrangement, including a thumb, a palm, and a finger region (see Fig. 1a). The catalytic cycle leading to nucleotide incorporation comprises several steps including a large structural rearrangement leading to a movement of the fingers towards the thumb region. In the first step, a 2′-deoxyribonucleoside-5′-triphosphate enters the active site of the DNA polymerase, forming an open substrate complex. Step 2 involves conformational changes to align the catalytic groups and to form a closed ternary complex. The nucleotidyl transfer reaction follows in step 3. The resulting product complex undergoes a reverse conformational change back to the open form (step 4), from which the pyrophosphate dissociates (step 5). The final translocation of the DNA strands leads back to the starting point for a new DNA synthesis cycle.

To maintain genomic integrity without the expensive proofreading performed by exonucleases, these polymerases have evolved a very high fidelity, with error frequencies of approximately 1 in 10^3–10^6 bases synthesised. However, given the demands of numerous biotechnological applications with their associated unnatural conditions, e.g. polymerase chain reactions (PCR), even this high degree of fidelity is not satisfactory. Such unnatural conditions either restrict the use of these enzymes or demand tedious optimisation steps. Thus, the primary design goal for DNA polymerases with altered functions is high specificity in the

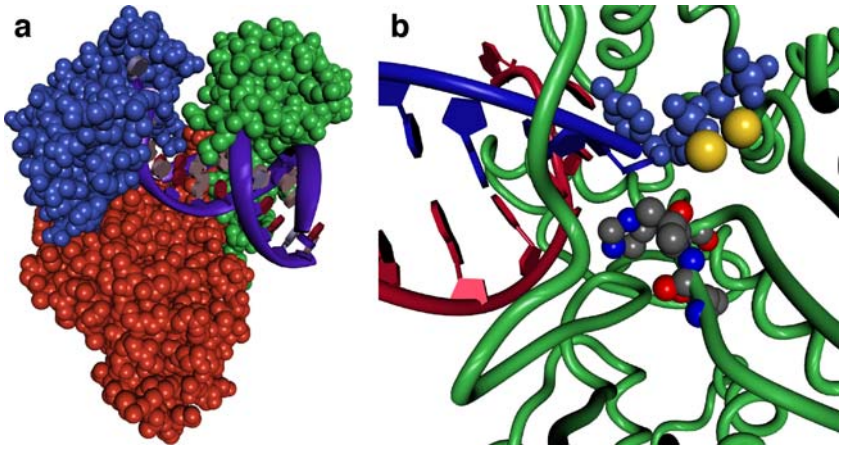

Fig. 1 **a** Hand-like structure of DNA polymerase I. The protein is shown in CPK model format with the palm in *red*, the thumb in *green*, and the fingers in *blue*. The DNA is depicted in ribbon representation. **b** Location of the three residues QVH, which were mutated to PLQ. The residues (colour coded by atom types), the incoming nucleotide (*blue*), and the magnesium ions (*yellow*) are depicted in CPK model format, and the remaining protein and DNA in ribbon representation (*green* protein, *red* template, *blue* primer)

formation of Watson-Crick base pairings during DNA synthesis. In this respect, Summerer et al. [1] developed an efficient automated high-throughput setup for the rapid parallel screening of DNA polymerase mutant libraries. With this technique, they constructed a library of 1,316 mutants of the Klenow fragment of *Escherichia coli* DNA polymerase I (KF^-) randomised at the consensus residues 879–881 (Q879, V880, and H881) (see Fig. 1b), which corresponds to residues 782–784 according to the numbering in the crystallographic determined complex structure 3KTQ [2] available from the Protein Data Bank [3] used as starting point in the calculations presented here. In the following, residue numbering is always according to the PDB entry. Several active variants, especially the three mutants PLQ, LVG, and LVL, with significant higher extension fidelity than the wild-type enzyme were identified in the library [1]. The new properties of mutated KF^- were then transferred to the thermostable *Thermus aquaticus* (*Taq*) DNA polymerase to provide tools that supercede the use of wild-type enzyme in highly accurate PCR-based genotyping techniques.

The goal of the work presented here was to analyse one of these mutants (PLQ) in terms of structural changes in order to rationalise this high specificity. On the atomic level, the exact kinetic mechanism of incorporation is still the subject of some debate even for the wild-type enzyme. Experimental studies have shown that, on the one hand, for the Klenow fragment the release of the polyphosphate is the slowest step in the case of a Watson-Crick pairing [4]. On the other hand, the barrier of the chemical reaction step is increased greatly for mismatches, making this step rate limiting [5]. But this behaviour can differ from one polymerase to the next. In recent years, a number of theoretical studies on different DNA polymerases have been published [6–21]. For example, it was shown that the chemical reaction and not the complex formation is rate limiting in the case of T7 DNA polymerase [17, 19, 20]. The fidelity can be attributed to deformations of the mismatched complexes leading to unfavourable starting structures for the chemical reaction. In this sense, Florian et al. [17, 19, 20] suggested that the incorporation of mismatched nucleotides takes place in a half-open form of T7 DNA polymerase, which causes a different reaction mechanism compared to the Watson-Crick incorporation revealed by free energy perturbation/empirical valence bond calculations. The group of Schlick [6, 9, 11, 14] showed that DNA polymerase β also cannot fully transform into the closed structure when incorporating a mismatched nucleotide. They even demonstrated in recent publications [9, 14] that the incorporation time of different nucleotides is correlated with the deformation of the active site, especially the coordination of the two magnesium ions.

Based on these published results, I decided to first concentrate on one specific mutant, PLQ, and the ternary complexes comprising the enzyme, the DNA primer and template as well as the incoming nucleotide before the chemical reaction. This will show that some of the selectivity of the mutant can already be explained by the different starting structures for the chemical reaction, leading probably to increased reaction barriers or even to totally different reaction pathways. Additionally, the well defined educt states will serve as starting points for future investigations on the reaction mechanism.

Materials and methods

In order to describe the differences in replication fidelity in atomic detail, molecular dynamics (MD) simulations were performed on the wild type and the PLQ mutant with Watson-Crick as well as mismatched base pairings of the incoming nucleotide. In this study, I describe results for an incoming desoxycytidine triphosphate (DCTP) opposite the Watson-Crick complementary guanosine (G) or a mismatched adenosine (A), cytidine (C), or thymidine (T).

Simulation details

The MD simulations were performed using the AMBER 8 suite of programs [22] with the modified version of the Cornell et al. force field (parm99) [23] for the protein, the DNA template and primer. The parameters for the polyphosphate were taken from the work of Meagher et al. [24] and those for magnesium from Aqvist [25]. The structure of the ternary complex in the closed form before incorporation of the new nucleotide was downloaded from the Protein Data Bank [3] (PDB entry 3KTQ [2]). The first three nucleotides of the primer and the last three of the template were deleted because they are very flexible [26], solvent exposed and not directly involved in binding. In this way, the computational demand could be decreased slightly. For the polymerase mutant, the corresponding amino acid side chains were removed and the backbone atoms renamed. The mismatched base pairs were generated by removing the base of the nucleotide of the template strand opposite the incoming nucleoside triphosphate and renaming the residue entry of the phosphate and the sugar group. During preparation of the input files for the MD simulations, the missing atoms, including those belonging to the side chains of the mutated amino acids and the mismatched base, were added in standard positions as defined in the AMBER parameter files using the tleap functionality [22]. With only three mutated residues, the fixed backbone, and the minimisation / constraint equilibration procedure described below, this procedure should give reasonable starting structures. These structures were then placed in a solvent box in the form of a periodic truncated octahedron. The distance between the edges of the water box and the closest atom of the solute was at least 12 Å in every direction. Sodium and chlorine ions were added to provide a physiological ionic strength of 0.15 mmol l^{-1} and to maintain electroneutrality.

The system was minimised by 8,000–10,000 steps to relax unfavourable conformations generated by the standard placement of the missing atoms. For equilibration, the system was then first heated from 100 K to 300 K for 100 ps and then relaxed to a density corresponding to 1 bar for 300 ps in a sequence of MD simulations using the canonical (NVT) and the isothermal isobaric (NPT) ensemble, respectively. In these simulations, harmonic restraints with force constants of 5 kcal mol^{-1} $Å^{-2}$ were applied to all solute atoms excluding the automatically added atoms. These restraints were then gradually reduced to zero during 200 ps of NVT-MD. Production runs of 30 ns were then performed. Again, these simulations used the canonical (NVT) ensemble, taking advantage of the fact that the pressure should not change dramatically in this type of simulation of a liquid system. Therefore, it was expected that the two ensembles (NPT and NVT) would give approximately the same results, with the additional advantage that the canonical ensemble minimises computational demand. The particle mesh Ewald (PME) method [27] was used in all simulations to treat long-range electrostatic interactions, and the SHAKE method [28] was used to constrain bond lengths of bonds involving hydrogen atoms. The time step for all MD simulations was set to 2 fs with a non-bonded cutoff of 9 Å.

Results and discussion

In this paper, I will concentrate on the incorporation of a cytosine (DCTP). Simulations were performed for this incoming nucleotide with all possible pairings with the four nucleotides in the template DNA strand for wild-type DNA polymerase I as well as the PLQ mutant. For each simulation, the last 10 ns were used for analysis. For this purpose, snapshots of the structures were taken every 2 ps and the water molecules, Na^+ and Cl^- ions were removed. For these snapshots, global structural changes, flexibilities, as well as interatomic distances were investigated. Additionally, all structures were aligned to the first structure of the time series and the atomic coordinates were averaged over all snapshots. The resulting average structures were minimised for 200 steps to generate valid bond lengths and angles.

Comparison between Watson-Crick and mismatched insertions in wild-type DNA polymerase I

The Watson-Crick as well as the mismatched insertions resulted in stable complex structures. This can be seen by the very small root mean square deviations (rmsd) of the C_α-atoms compared to the average structure (see Fig. 2). For all complexes, these rmsd values are around 1 Å for all time steps. Only for the Watson-Crick base pairing, there were somewhat larger deviations of up to 1.6 Å in the very last

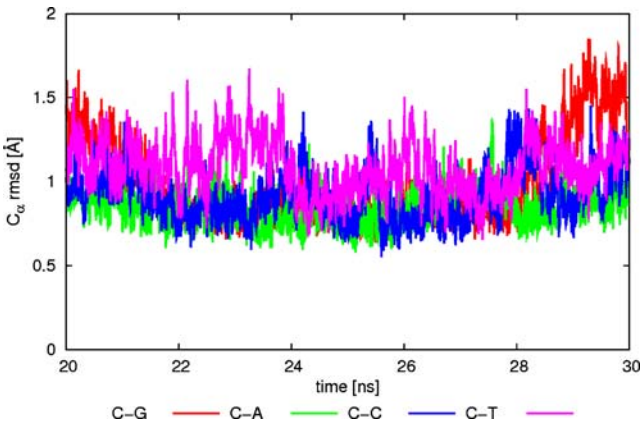

Fig. 2 Root mean square deviation (rmsd) of the C_α-atoms of DNA polymerase I with different base pairings of DCTP for the last 10 ns of a 30 ns molecular dynamics (MD) simulation

nanosecond of the simulation. This is due to a movement of the thumb upwards relative to the finger region (see Fig. 3a). If one follows the simulations for up to 40 ns [see Fig. S1 in the Electronic Supplementary Material (ESM)], it can be seen that, after around 32 ns, the structure reverts to a structure very similar to that present before the upwards move of the thumb. Additionally, it is worth mentioning that this upwards movement does not change the distance between helix 32 of the fingers and the thumb [measured as the distance between (Lys508-C_α–Ala743-C_α, see Fig. 3b and Fig. S3], which is the major change between the complexes with Watson-Crick and mismatched base pairs (see below). Thus, this movement represents a larger fluctuation around the optimal structure but has little influence on the active site.

When comparing the average structures of the four complexes, it becomes evident that they all have a very similar global conformation (see Fig. 4). The rmsd values compared to the C–G complex are 1.30 Å, 1.30 Å, and 1.53 Å for the C–A, C–C, and C–T mismatch, respectively. Only in the thumb region and parts of the finger (beginning of helix 23: residues 738–747) region larger deviations can be observed. In the case of the C–A and C–C mismatch, the thumb is rotated away from the fingers. In the C–T case, the thumb is again translated upwards but even more strongly than in the last nanosecond of the C–G match.

In order to quantify these changes, the distance from the beginning of helix 23 in the finger region to the nearest loop of the thumb (residue 506–510) was measured. In the mismatched structures, an opening of this distance of around 2 Å is observed (Lys508-C_α–Ala743-C_α distance, see Table 1 and Fig. S3). If the distance is calculated to the first turn of helix 32 (Lys508-C_α–Ser739-C_α), the difference is even larger than 5 Å. But this can be attributed mainly to the high flexibility of this first turn, as evidenced by the large standard deviation (see Table 1) and the fast and large fluctuations of this distance (see time series in Fig. S4). If the locations of the side chains are also considered, all these deviations lead to additional space for the DNA template and primer in the active site of the mismatched complexes (see Fig. S5). In contrast, the mismatches do not lead to any changes in the relative orientation of helix 18 (see also Table 1). The large rotation of this helix distinguishes the open from the closed, reactive form of DNA polymerase I. Thus, all complexes represent the closed form and the assumption that the reaction starts from a half-open form in the mismatched complexes, as suggested by other groups [6, 9, 11, 14, 17, 19, 20], cannot be reproduced in the study presented here.

Despite the differences mentioned above, the conformation of DCTP is almost identical in all complexes (see Figs. S7, S8). The only differences are some readjustments of the positioning of the incoming base and the immediately adjacent bases to facilitate the strongest possible hydrogen-bonding and π-stacking interactions. Therefore, the investigations conducted here are unable to explain the fidelity of the wild-type enzyme. Due to the limitations of classical MD, the results presented here show only the formed complex before the chemical reaction, which seems to be very similar for all matching and mismatching base pairings. One possible influence on the reaction rates and, therefore, on the fidelity could be the additional space for the DNA described above, which could be responsible for a decrease in the reaction speed in mismatched complexes. The enzyme forces the substrates into a conformation similar to the transition state of the reaction, which is not very effective if there is additional space into which the substrates can "escape". It is planned to verify this hypothesis in subsequent work using calculations of the relative activation energies for the chemical reaction in matched and mismatched cases using a quantum mechanical/molecular mechanical (QM/MM) approach. For example, for T7 DNA polymerase, such calculations showed very good correlation with the experimental reaction rates [20].

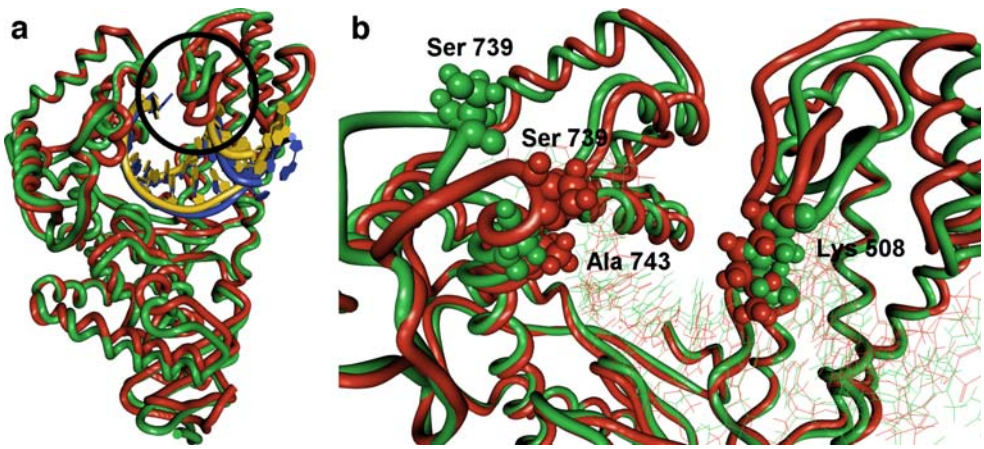

Fig. 3 **a** Comparison of the structure of wild-type DNA polymerase I after 20 ns (*red / blue*) and 30 ns (*green / yellow*) of MD simulation. The upwards movement of the thumb is highlighted by the *circle*. **b** Amino acids (CPK model) used in the distance calculation of helix 23 and the thumb region: the structure of the complex with the mismatched base pairing C–G is shown after 20 ns (*red*) and 30 ns (*green*) of MD simulation. The large flexibility of the first turn of helix 23 can be observed easily

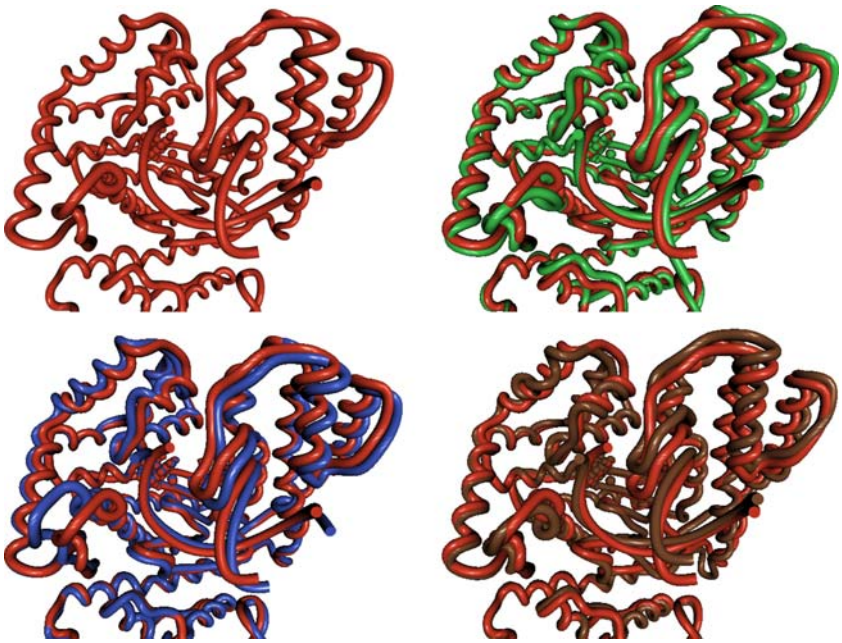

Fig. 4 Backbone of wild-type DNA-polymerase I with the Watson-Crick C–G (*red*), C–A (*green*), C–C (*blue*), and C–T (*brown*) base pairing

Comparison between wild-type DNA polymerase I and the PLQ mutant

When Watson-Crick base pairing is compared in the wild-type and the mutant, differences in the positioning of the thumb region can also be seen (see Fig. 5). This can again be quantified by the Lys508-C_α–Ala743-C_α distance, which is more than 4 Å larger in the mutant compared to the wild type (Table 2). This gives the DNA template and primer even more space, which probably further decreases the reaction rate (see discussion above). It is often observed that selectivity and efficiency are inversely correlated in catalysis. Thus, a higher fidelity caused by a lower efficiency is not unexpected. Unfortunately, no experimental data to verify this hypothesis are available.

The mutations have almost no influence on the positioning of the DCTP (Fig. S9). Also, no changes in the primer and the template are observed. Nevertheless, the mutations have a strong influence on the interactions of the enzyme with the DNA primer. His784 and, especially, Gln582 interact strongly with the primer close to the incorporation site. Gln582 builds a hydrogen bond to a cytosine (C111) in the primer, one base away from the reaction site (see Fig. 6a). In the mutated polymerase, Gln784 does not interact so favourably with the primer as does His784. Additionally, and even more interestingly, the Gln582–C111 hydrogen bond is broken. In contrast, two new hydrogen bonds are formed to the backbone of Pro782 and the side chain of Gln784 (see Fig. 6b). These hydrogen bonds seem to be more favourable than the one to C111. In summary, the mutations lead to weaker interactions of the enzyme with the primer and, in this way, to an ineffectual fixation of the primer with more space to adjust to the incoming nucleotide (see below).

Comparison between Watson-Crick and mismatched insertions in the PLQ mutant

For the mismatches in the PLQ mutant, once again very similar overall structures can be seen (Fig. 5). The opening between helix 23 and the nearest loop of the thumb (residue 506–510) is, expect for C–T, almost identical to the mutated

Table 1 Distances (in Å) and corresponding standard deviations (in brackets) between C_α atoms of different amino acids in the finger and thumb regions from all snapshots of the last 10 ns of the molecular dynamics (MD) simulation

Atoms	Wild type C-G	Wild type C-A	Wild type C-C	Wild type C-T	Closed form 3KTQ	Open form 2KTQ
Lys508–Ala743	12.1 (1.3)	14.0 (0.9)	14.1 (1.3)	14.2 (1.2)	16.4	16.1
Lys508–Ser739	10.0 (1.6)	12.0 (1.1)	15.4 (1.9)	13.1 (2.5)	15.2	14.8
Arg587–Leu657	7.3 (0.3)	7.3 (0.3)	7.0 (0.5)	7.0 (0.4)	7.2	21.2

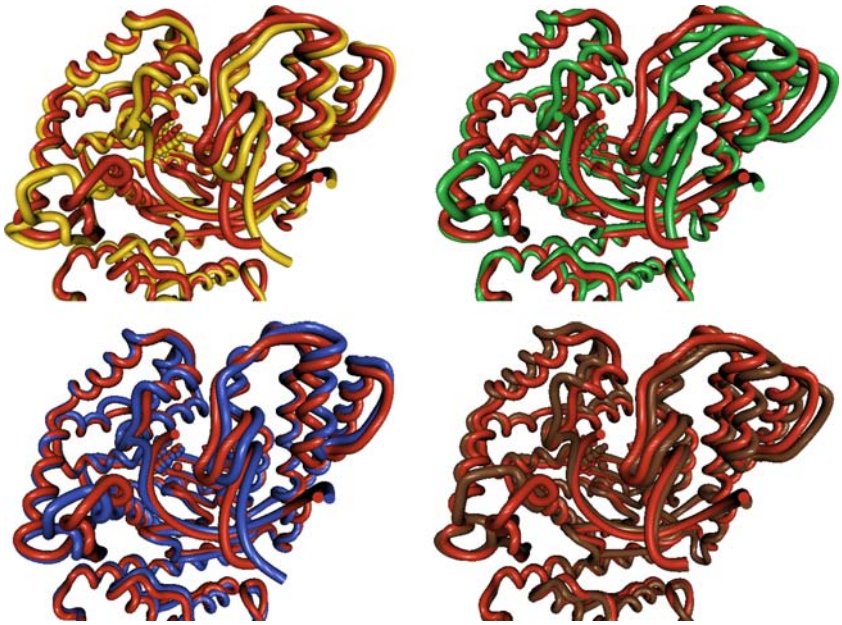

Fig. 5 Backbone of the PLQ mutant with the Watson-Crick C–G (*yellow*), C–A (*green*), C–C (*blue*), and C–T (*brown*) base pairing in comparison to the wild-type enzyme (*red*, C–G base pair)

complex with the Watson-Crick base pairing, and consequently larger than in the corresponding wild type complexes (Table 2). But a closer look at the surroundings of the DCTP reveals the major differences (see Fig. 7). Although the nucleotide has almost the same orientation as in the Watson-Crick case, the most obvious adaptation to the mismatch is that the DNA primer moves away from the triphosphate and the magnesium ion in two out of the three mismatches. As shown in Table 3 (see also time series in Fig. S11), the distance between O_3' of the primer and the magnesium ion has almost doubled in the C–A and C–C mismatch. These specific atoms have to be brought as close together as possible during the chemical reaction, explaining the additional reduction in the incorporation rate of the mismatches. A number of reasons for the displacement can be observed, each of which being more or less dominant in the different complexes. As discussed in the previous section, substitution of the His by a Gln side chain is of especially major importance. While in the wild type, His784 and Gln582 interact with the DNA primer, forcing it into the correct position for the reaction, in the mutant Gln784 and Gln582 interact with each other (C–G and C–A base pairing). Although the conformation of this interaction in the complex differs between the mismatched and the Watson-Crick base pair, the fixation of the primer is weakened and, in this way, the end of the primer is not efficiently forced into a favourable conformation for the chemical reaction.

Another important factor is Arg573 (Fig. 8). While in the wild type this amino acid builds at most only a very weak hydrogen bond with the O2 of the last base of the primer (C112) due to steric hindrance with His784, this hydrogen bond is strengthened in the mutant (expect in the case of Watson-Crick pairing) and the primer end responds to this additional pull. In the C–A case, an influence of this changed environment on the incoming DCTP can be clearly seen. The non-optimal hydrogen-bonding network between primer and template allows for a rotation of the incoming base so that the O2 of DCTP forms another hydrogen bond with A573. In the other two mismatches, this movement is not observed. Reasons for this could be that Gln784 has not moved out of the way (yet) to permit this interaction, and/or that the interactions within the base pairing do not permit the rotation so easily.

Only in the C–T mismatch are the P_α-O_3' distances in the same range as in the Watson-Crick C–G case. Thus, fidelity cannot be explained on the basis of the pre-reaction complex in this case. On the one hand, a hydrogen bond is

Table 2 Distances (in Å) and corresponding standard deviations (in brackets) between C_α atoms of different amino acids in the fingers and thumb region from all snapshots of the last 10 ns of MD simulation

Atoms	Mutant C-G	Mutant C-A	Mutant C-C	Mutant C-T	Wild Type C-G
Lys508–Ala743	16.4 (1.1)	16.0 (1.6)	16.0 (1.1)	14.0 (0.9)	12.1 (1.3)
Lys508–Ser739	18.2 (1.6)	18.3 (3.2)	13.8 (1.4)	14.3 (1.1)	10.0 (1.6)
Arg587–Leu657	7.3 (0.4)	7.0 (0.4)	6.8 (0.3)	7.1 (0.6)	7.3 (0.3)

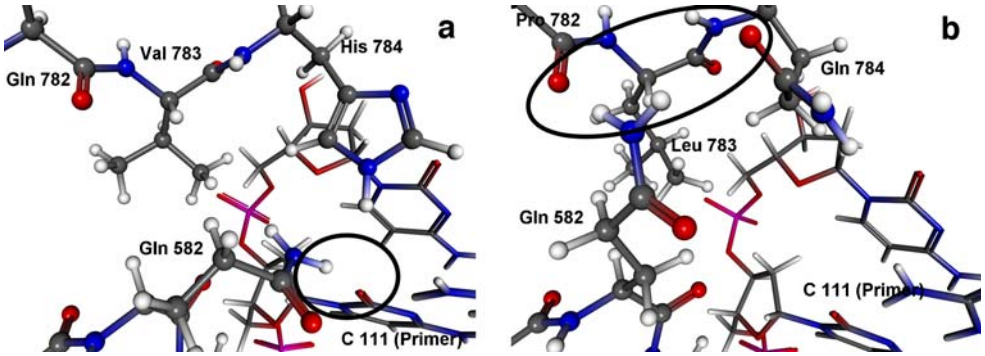

Fig. 6 Interactions of **a** Gln782, Val783 and His784 and **b** the mutated Pro782, Leu783 and Gln784 with the DNA primer as well as Gln582 in the wild-type enzyme and mutant, respectively. While Gln582 interacts strongly with the primer in the wild type, it builds hydrogen bonds to Pro782 and Gln784 in the mutant (*circled areas*)

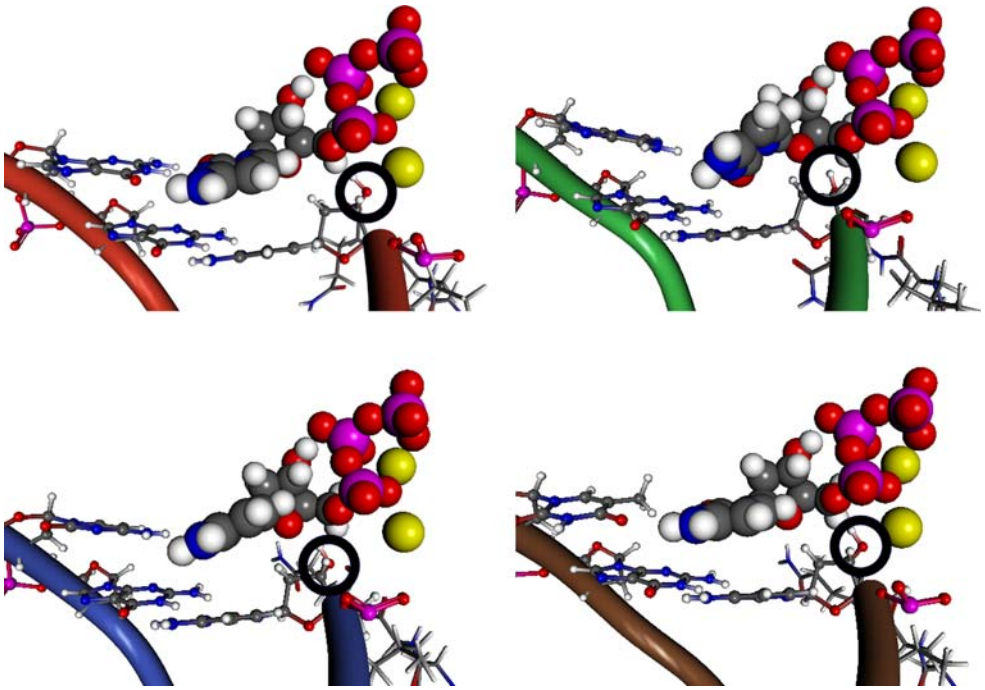

Fig. 7 Conformation of DCTP in the PLQ mutant of DNA polymerase I. *Upper left* Watson-Crick (C–G), *upper right* C–A, *lower left* C–C, *lower right* C–T. The O_3' of the primer is marked by a *circle*

Table 3 Atom–atom distances (Å) in the ternary complex of wild type DNA polymerase I and a mutant for the Watson-Crick and mismatched incoming nucleotide. If equivalent atoms exist, the shorter distance is used for each snapshot (NH1 and NH2 in Arg)

Atoms	Wild Type C-G	Wild Type C-A	Wild Type C-C	Wild Type C-T
P_α-O_3'	3.2 (0.1)	3.1 (0.1)	3.2 (0.2)	3.1 (0.1)
Mg_A-O_3'	2.3 (0.2)	2.2 (0.1)	2.4 (0.4)	2.2 (0.2)
NH(Arg573)-O2(C112)	4.8 (0.5)	4.6 (0.3)	5.0 (0.8)	2.8 (0.1)
NH(Arg573)-O2(DCPT)	4.9 (0.3)	5.1 (0.3)	4.7 (0.4)	4.8 (0.3)
Atoms	Mutant C-G	Mutant C-A	Mutant C-C	Mutant C-T
P_α-O_3'	3.1 (0.1)	4.1 (0.2)	3.7 (0.5)	3.1 (0.1)
Mg_A-O_3'	2.2 (0.1)	4.5 (0.2)	3.5 (1.0)	2.2 (0.1)
NH(Arg573)-O2(C112)	5.9 (0.5)	2.8 (0.2)	3.3 (0.7)	3.6 (0.7)
NH(Arg573)-O2(DCPT)	5.3 (0.4)	2.9 (0.2)	6.1 (1.2)	6.0 (0.5)
NE2(Gln582)-OE1(Gln784)	3.7 (0.4)	3.1 (0.4)	9.1 (0.7)	9.5 (0.6)
OE1(Gln582)-NE2(Gln784)	3.3 (0.4)	6.2 (0.3)	8.1 (0.5)	9.1 (0.6)

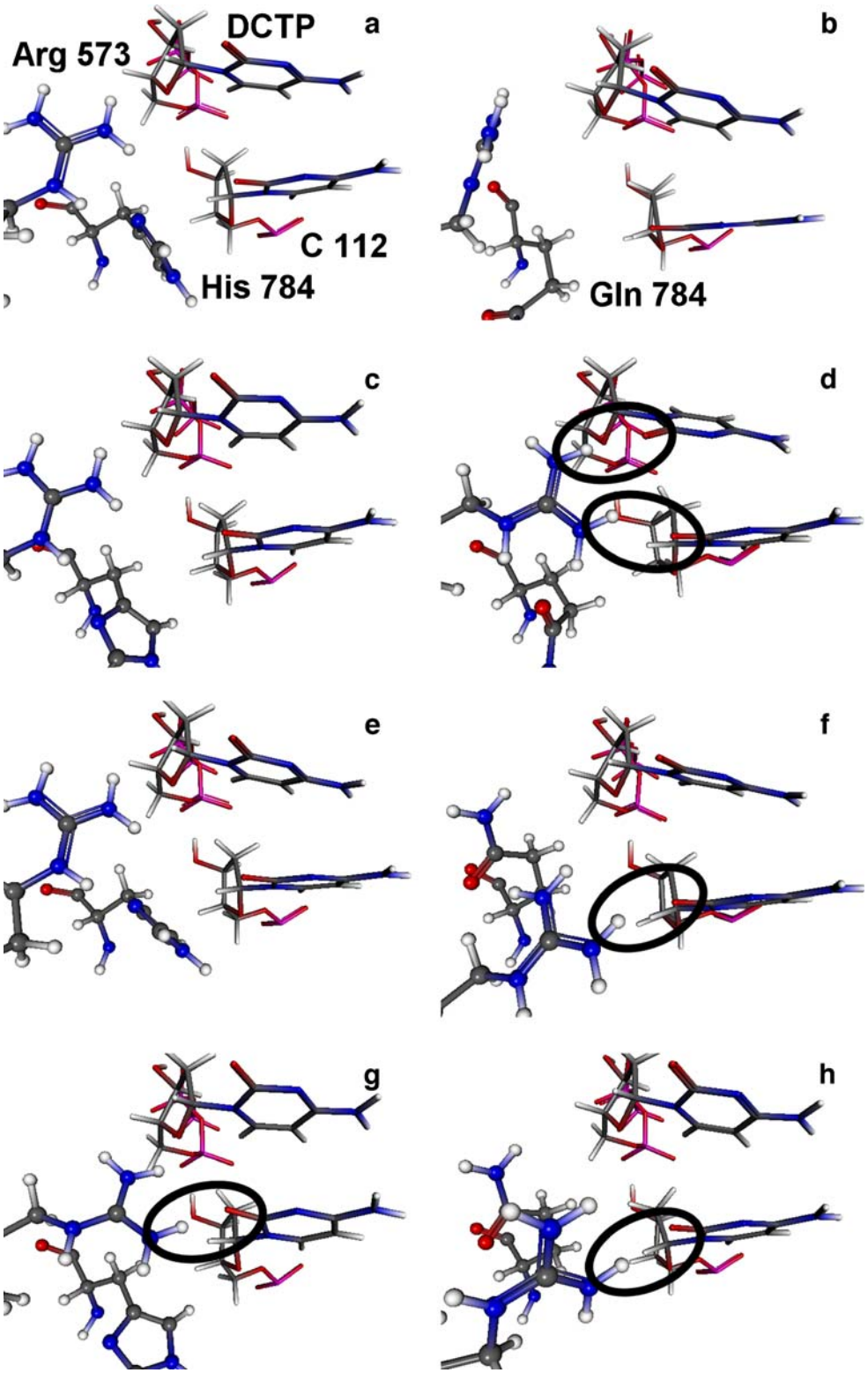

Fig. 8 Interactions between Arg573, DCTP and C112 of the DNA primer in the wild type (**a**–**d**) and the mutant (**e**–**h**): **a**, **e** C–G; **b**, **f** C–A; **c**, **g** C–C; **d**, **h** C–T. Hydrogen bonds are marked by *ellipses*

observed from Gln582 to C111 but not to any of the bases in the mutated triad, which is the same arrangement as in the C–G case. On the other hand, a hydrogen bond is formed between C112 and Arg573 as in the other mismatches. Interestingly, this hydrogen bond is observed in the wild type only for this mismatch. Nevertheless, there is the possibility that these distinctions of C–T are artifacts of the simulation resulting from insufficient sampling. This becomes evident from the C–C mismatch, in which the displacement of the primer does not occur until 24 ns of

MD simulation have passed (Fig. S11), and from the large standard deviations in the C–C and C–T cases (Table 3).

With all these interactions influencing the location of the DNA primer, it is worth mentioning once again how little the hydrogen bonding network between the mismatched base pairs (incoming DCTP with mismatched base A/C/T204) is affected (see Fig. S12). In the C–A pair, the rotation of the DCTP, which is caused by the additional pull of Arg573, can be seen in the mutant. But the only major change in the hydrogen-bonding network is the 180° rotation of T204 in the mutant. But this is not a direct result of the mutated amino acids, which lie far away from the DNA template and thus no direct interaction can occur (Fig. S13). In the mutant enzyme, a hydrogen bond is built between T204 and Arg677, which seems only to be possible due to the lesser degree of restriction of the active site in the mutant. In contrast, the optimal hydrogen-bonding network is formed between the bases in the wild type because the more favourable interaction with the enzyme is sterically forbidden.

Conclusions

This study investigated the fidelity of a mutant of DNA polymerase I by means of MD simulations. In this mutant, amino acids at sites 782–784 (Gln782, Val783, and His784, consensus sites 879–881) according to the numbering in the crystallographic determined complex structure 3KTQ [2] used as the starting point for the calculations presented here, are replaced by Pro782, Leu783, and Gln784, respectively. Ternary complexes comprising enzyme, DNA primer and template as well as the incoming nucleotide before the chemical reaction were simulated for the wild-type and the mutated enzyme. These simulations show that high fidelity is not primarily due to the direct interaction of the mutated amino acids with the incoming nucleotide or the DNA primer and template. However, the different interactions especially of Gln784 with two adjunct residues, lead to significant changes in the relative orientations of partners in the complex. While Gln582 interacts with the DNA primer in the wild type, it can build a hydrogen bond with Gln784 in the mutant, weakening binding of the DNA. In contrast, Arg573 builds stronger interactions with the primer and the incoming nucleotide in the mutant than in the wild type, especially in complexes with mismatched base pairings C–A and C–C. These differences cause the DNA primer to move away from the triphosphate and the magnesium ion in these two mismatches. Because one of the main features of the enzyme is to bring the O_3' of the primer and the phosphate group of the incoming nucleotide as close together as possible to resemble the transition state of the reaction, the structure of the complex before the reaction can already partly explain the high fidelity of the PLQ mutant in these two complexes. In comparison with simulations performed on other DNA polymerases [6–21], the main difference is that, in DNA polymerase I, the complexes with mismatched base pair can also form closed ternary structures, even if these are sometimes distorted regarding the relative orientation of the DNA primer and the incoming nucleotide. For T7 DNA polymerase [17, 19, 20] and DNA polymerase β [6, 9, 11, 14], only part-closure to half open structures was proposed for mismatches, leading to an altered reaction mechanism. In the same sense, the results presented here lead to the conclusion that, in the mutant DNA polymerase I, the distortions (although occurring for different reasons) may also modify the reaction mechanism. But whether the finding that the chemical reaction is the rate-limiting step as in T7 DNA polymerase [17, 19, 20] can be transferred to DNA polymerase I remains to be proven. Further investigations into the reaction mechanism using the structures obtained here as a starting point are in progress in order to determine the influence of the mismatches on the transition state and the reaction rates.

Acknowledgements I would like to thank Andreas Marx, University of Konstanz, for constructive discussions and proofreading of the manuscript. I also thank the Common Ulm Stuttgart Server (CUSS) and the Baden-Württemberg grid (bwGRiD), which is part of the D-Grid system, for providing the computer resources making the simulations possible. Additionally, my special thanks go to the anonymous reviewers for their helpful suggestions for improving the paper.

References

1. Summerer D, Rudinger NZ, Detmer I, Marx A (2005) Angew Chem Int Ed 44(30):4712–4715
2. Li Y, Korolev S, Waksman G (1998) EMBO J 17:7514–7525
3. Berman HM, Westbrook J, Feng Z, Filliland G, Bhat TN, Weissig H, Shindyalov IN, Bourne PE (2000) Nucleic Acids Res 28(1):235–242
4. Kuchta RD, Mizrahi V, Benkovic P, Johnson KA, Benkovic SJ (1987) Biochemistry 26:8410–8417
5. Eger BT, Benkovic SJ (1992) Biochemistry 31:9227–9236
6. Yang L, Beard WA, Wilson SH, Roux B, Broyde S, Schlick T (2002) J Mol Biol 321:459–478
7. Yang L, Beard WA, Willson SH, Broyde S, Schlick T (2002) J Mol Biol 317:651–671
8. Yang L, Beard WA, Willson SH, Broyde S, Schlick T (2004) Biophys J 86:3392–3408
9. Arora K, Schlick T (2004) Biophys J 87(5):3088–3099
10. Yang L, Arora K, Beard WA, Wilson SH, Schlick T (2004) J Am Chem Soc 126:8441–8453
11. Radhakrishnan R, Schlick T (2005) J Am Chem Soc 127:13245–13252
12. Radhakrishnan R, Schlick T (2004) Proc Natl Acad Sci USA 101 (16):5970–5975
13. Arora K, Schlick T (2005) J Phys Chem B 109:5258–5367
14. Arora K, Beard WA, Willson SH, Schlick T (2005) Biochemistry 44(40):13328–13341

15. Radhakrishnan R (2006) Biochem Biophys Res Comm 347:626–633
16. Florián J, Warshel A, Goodman MF (2002) J Phys Chem B 106:5739–5753
17. Florián J, Warshel A, Goodman MF (2002) J Phys Chem B 106:5754–5760
18. Florián J, Goodman MF, Warshel A (2003) Biopolymers 68:286–299
19. Florián J, Goodman MF, Warshel A (2003) J Am Chem Soc 125:8163–8177
20. Florián J, Goodman MF, Warshel A (2005) Proc Natl Acad Sci USA 102(19):6819–6824
21. Rittenhouse RC, Apostoluk WK, Miller JH, Straatsma TP (2003) Proteins 53:667–682
22. Case DA, Darden TA, Cheatham TEIII, Simmerling CL, Wang J, Duke RE, Luo R, Merz KM, Wang B, Pearlman DA, Crowley M, Brozell S, Tsui V, Gohlke H, Mongan J, Hornak V, Cui G, Beroza P, Schafmeister C, Caldwell JW, Ross WS, Kollman PA (2004) Amber 8. University of California, San Francisco, CA
23. Cornell WD, Cieplak P, Bayby CI, Gould IR, Merz KM, Ferguson DM, Spellmeyer DC, Fox T, Caldwell JW, Kollman PA (1995) J Am Chem Soc 117:5179–5197
24. Meagher KL, Redman LT, Carlson HA (2003) J Comp Chem 24:1016–1025
25. Aqvist J (1992) J Mol Struct 88:135–152
26. Exner TE (2007) Comparison of the incorporation of Watson-Crick complementary and mismatched nucleotides catalyzed by DNA polymerase I. In: Nagel WE, Kröner DB, Resch M (eds) High performance computing in science and engineering '07, transactions of the high performance computing center, Stuttgart (HLRS) 2007. Springer, Berlin, pp 187–199
27. Darden T, York D, Pedersen L (1993) J Chem Phys 98:10089–10092
28. Ryckaert JP, Ciccotti G, Berendsen HJC (1977) J Comput Phys 23:327–341